tvst

Pediatric Ophthalmology & Strabismus

A Dosage-Dependent Dominant-Negative Mechanism of SLC45A2(W74R) in Autosomal Dominant Oculocutaneous Albinism Revealed by Zebrafish Modeling

Dongheon Surl[1,*], Tae-Ik Choi[2,*], Ji-Won Park[2], Dilan Wellalage Don[2], Tae Young Kim[3], Mervyn G. Thomas[4], Jong-Su Park[5], Xiangyun Wei[5], Young-Ki Bae[6], Jinu Han[7], and Cheol-Hee Kim[2]

[1] Institute of Vision Research, Department of Ophthalmology, Yongin Severance Hospital, Yonsei University College of Medicine, Yongin, South Korea
[2] Department of Biology, Chungnam National University, Daejeon, South Korea
[3] Institute of Vision Research, Department of Ophthalmology, Gangnam Severance Hospital, Yonsei University College of Medicine, Seoul, South Korea
[4] The University of Leicester Ulverscroft Eye Unit, School of Psychology and Vision Sciences, University of Leicester, Leicester, UK
[5] Departments of Ophthalmology and Microbiology & Molecular Genetics, University of Pittsburgh School of Medicine, Pittsburgh, PA, USA
[6] Research Institute, National Cancer Center, Goyang-si, Gyeonggi-do, South Korea
[7] Institute of Vision Research, Department of Ophthalmology, Severance Hospital, Yonsei University College of Medicine, Seoul, South Korea

Correspondence: Jinu Han, Institute of Vision Research, Department of Ophthalmology, Severance Hospital, Yonsei University College of Medicine, 50-1 Yonsei-ro, Seodaemun-gu, Seoul 03722, South Korea. e-mail: jinuhan@yuhs.ac
Cheol-Hee Kim, Department of Biology, Chungnam National University, 99 Daehak-ro, Yuseong-gu, Daejeon 34134, South Korea. e-mail: zebrakim@cnu.ac.kr

Received: July 29, 2025
Accepted: January 14, 2026
Published: February 18, 2026

Keywords: oculocutaneous albinism; *SLC45A2*; autosomal dominant; zebrafish; knockout

Citation: Surl D, Choi TI, Park JW, Don DW, Kim TY, Thomas MG, Park JS, Wei X, Bae YK, Han J, Kim CH. A dosage-dependent dominant-negative mechanism of SLC45A2(W74R) in autosomal dominant oculocutaneous albinism revealed by zebrafish modeling. Transl Vis Sci Technol. 2026;15(2):22, https://doi.org/10.1167/tvst.15.2.22

Purpose: To investigate the clinical characteristics of autosomal dominant oculocutaneous albinism (OCA) and functionally validate the heterozygous SLC45A2(W74R) variant using a zebrafish model.

Methods: Three members of a Korean family with OCA underwent comprehensive clinical examinations. Targeted panel and genome sequencing were performed on the proband, and Sanger sequencing was performed on all affected family members. To assess the pathogenicity of the genetic variant, a *slc45a2* knockout (KO) zebrafish model was generated using CRISPR technology.

Results: All three affected patients exhibited hair and iris hypopigmentation, with variable foveal hypoplasia and nystagmus. A heterozygous c.220T>C:p.(W74R) variant in *SLC45A2* was identified and was absent in gnomAD v4.1. Multiple in silico predictions supported its pathogenicity (AlphaMissense: 0.993, CADD: 29.6, REVEL: 0.951). Genome sequencing revealed no additional pathogenic or common hypomorphic variants in other known OCA-related genes. The *slc45a2* KO zebrafish exhibited a typical albino phenotype, which was rescued by melanocyte-specific expression of normal *SLC45A2* but not by the *SLC45A2*(W74R) variant. Furthermore, the *SLC45A2*(W74R) variant suppressed pigmentation in heterozygous KO, but not in wild-type zebrafish, indicating a dominant-negative effect in a dosage-dependent manner.

Conclusions: This study demonstrated that a heterozygous c.220T>C:p.(W74R) variant in *SLC45A2* causes variable expressivity of OCA in a dominant inherited manner, and this variant interferes with melanogenesis in zebrafish.

Translational Relevance: This study expands the mode of inheritance in OCA and provides crucial functional validation that is important for genetic counseling.

Introduction

Oculocutaneous albinism (OCA) is a genetically heterogeneous disorder characterized by a reduction or complete absence of melanin pigments in skin, hair, and eyes. This heterogeneity arises from pathogenic variants not only in genes directly involved in the melanin production and processing within melanocytes but also in those critical for upstream and supporting processes, including neural crest formation, melanocyte development, melanosome biogenesis and trafficking, and pigment-related signaling pathways.[1] To date, mutations in eight genes have been associated with ocular albinism (OA) or OCA, while 15 genes have been identified in syndromic OCA.[2] Among the eight types of nonsyndromic OCA (OCA1–8), seven causative genes have been identified, and OCA5 has been mapped to the 4q25 locus in a consanguineous Pakistani family.[3] Ophthalmologic features of OCA include infantile nystagmus, iris transillumination defects, varying degrees of foveal hypoplasia, hypopigmented fundi, chiasmal misrouting of the optic nerve, poor stereopsis, and decreased visual acuity.[4–6]

The estimated prevalence of OCA is about 1 in 17,000 to 20,000 in Western countries,[5] while in Africa, it ranges from 1 in 5,000 to 1 in 15,000.[7] Among the known causative genes, *TYR* is the most frequently mutated gene, accounting for 42% of all OCA cases, while *SLC45A2* mutations are a common cause of OCA, particularly OCA4 in East Asia.[8,9] *SLC45A2* is composed of seven exons and encodes a membrane-associated transporter protein of 530 amino acids with 12 putative transmembrane domains.[10] SLC45A2 protein plays a key role in neutralizing melanosome pH and facilitating copper binding to tyrosinase.[11]

In this study, we identified a novel *SLC45A2* variant, *SLC45A2*(W74R), responsible for autosomal dominant OCA4 in three patients from a single family. OCA4 is typically inherited in an autosomal recessive pattern, requiring two copies of the mutated *SLC45A2* (one from each parent) for disease manifestation. To assess the pathogenicity of this *SLC45A2* variant, we generated a *slc45a2* knockout (KO) zebrafish and found an experimental clue suggesting a dominant-negative effect with dosage-dependent activity of this variant offering new insights into the molecular mechanism underlying OCA4.

Materials and Methods

Ethical Approval and Consent

The study adhered to the tenets of the Declaration of Helsinki, and institutional review board (IRB) approval was obtained from Gangnam Severance Hospital IRB (No. 3-2021-0153). Patient consent was obtained for the publication of clinical data and photographs.

Genetic Analysis

Targeted panel next-generation sequencing, consisting of 429 genes (listed in Supplementary Table S1) associated with inherited eye diseases, was performed using NextSeq 550 (Illumina, San Diego, CA, USA). Target enrichment was carried out with custom-designed RNA oligonucleotide probes and a target enrichment kit (Celemics, Seoul, South Korea). Genome sequencing of the proband was performed using PCR-free TruSeq on a NovaSeq 6000 (Illumina). Demultiplexed BAM files were aligned to the hg38 reference genome using Dragen mapper. Single-nucleotide variants and small insertions or deletions were identified using the Genome Analysis ToolKit (GATK) version 4.4.4.0 with HaplotypeCaller. Each variant suspected to be pathogenic, likely pathogenic, or a variant of uncertain significance was confirmed by visual inspection of the BAM file using Integrative Genomics Viewer 2.16 software. Structural variants were called with the GATK-SV cohort mode pipeline with cn.Mops, GATK gCNV, Manta, Wham, and SCRAMble.[12] The mobile element insertion was analyzed using the MELT algorithm.[13] Causative genes for nonsyndromic or syndromic albinism were selected for the analysis. Variants with combined annotation dependent depletion (CADD) <20 and a minor allele frequency (MAF) >0.5% in the Genome Aggregation Database (gnomAD v4.1) were excluded during the initial filtering pipeline. To identify known common hypomorphic variants affecting skin pigmentation, we specifically searched those variants without MAF filtering in *TYR*.[14] The potential pathogenicity of each variant was determined according to the guidelines of the American College of Medical Genetics and the Association for Molecular Pathology,[15] and three in silico prediction algorithms, including Alphamissense, CADD, PolyPhen-2, REVEL, Sorting Intolerant From Tolerant (SIFT), and VEST4 (Variant Effect Scoring Tool), were used for pathogenicity prediction.[16] Protein modeling was performed using Alphafold 3 Server and UCSF ChimeraX.[17] To perform a haplotype analysis of *SLC45A2* in the proband, the phase of each variant was determined directly from paired-end sequence read pairs or imputed using the SEAD reference panel, which includes 22,134 haplotypes from Asian populations (https://imputationserver.westlake.edu.cn).[18]

Ophthalmologic Examination

Patients underwent comprehensive ophthalmologic examinations, including measurement of visual acuity, slit-lamp examination, manifest refraction, dilated fundus examination, fundus photograph (VX-20; KOWA, Tokyo, Japan), wide-field fundus photography (Optos, Marlborough, MA, USA), and Spectralis optical coherence tomography (OCT, Heidelberg Engineering GmbH, Heidelberg, Germany). Multichannel visual evoked potential (VEP) was used to assess the misrouting of retinal ganglion cell axons at the optic chiasm with pattern onset/offset stimulus. Video nystagmography (SLMED, Seoul, South Korea) was performed to record eye movements. Funduscopic evaluation of macula status and foveal hypoplasia was conducted based on the Foveal Hypoplasia Grading Scale.[19]

In vivo Characterization in Zebrafish

Zebrafish Husbandry

Zebrafish were reared under standard conditions with a 14-hour/10-hour light/dark cycle. Zebrafish embryos were obtained by natural mating and reared in egg water at 28.5°C. Developmental stages of the organogenesis period are represented as hours postfertilization (hpf). Wild-type and KO zebrafish were obtained from the Zebrafish Center for Disease Modeling. Animal experiments involving zebrafish were approved by the Institutional Animal Care and Use Committees of Chungnam National University (202404A-CNU-077) and adhered to the ARVO Statement for the Use of Animals in Ophthalmic and Vision Research.

Plasmid Construction

The wild-type *SLC45A2* was obtained from GenScript (clone ID: OHu107237) and subcloned into the pCS2$^+$ expression vector. The *SLC45A2*(Y70H) and *SLC45A2*(W74R) variants were introduced by site-directed mutagenesis using the pCS2$^+$*SLC45A2* expression vector as a template. To achieve tissue-specific expression of *SLC45A2*, we constructed a vector containing the melanocyte-specific *fTyrp1* promoter, ZsGreen1 reporter gene, P2A peptide, and *SLC45A2* using the NEBuilder HiFi DNA Assembly Cloning Kit (#E5520; New England Biolabs, Ipswich, MA). We employed a bicistronic linker, P2A, which enables to coexpress ZsGreen1 and SLC45A2 in same transgene-positive cells. Briefly, the *fTyrp1* promoter, ZsGreen1-P2A, and *SLC45A2* cDNA were polymerase chain reaction (PCR)–amplified with overlapping ends. The PCR products were then assembled into a *NcoI* digested pCS2$^+$ vector using the HiFi DNA Assembly kit according to the manufacturer's instructions. The resulting plasmids were verified by Sanger sequencing. The detailed primer sequences used in the construction are provided in Supplementary Table S2.

Generation of Zebrafish *slc45a2* KO Mutants

To generate zebrafish *slc45a2* KO mutants, we designed single guide RNAs (sgRNAs) targeting exon 1 of the zebrafish *slc45a2* gene using CRISPRScan (https://www.crisprscan.org/). In vitro transcription of sgRNA was performed using the MAXIscript T7 Transcription Kit (AM1314; Invitrogen, Carlsbad, CA, USA). Cas9 expression vector (pT3TS-nCas9n) was linearized with *XbaI* (R0145; NEB), and Cas9 messenger RNA (mRNA) was transcribed using the mMESSAGE mMACHINE T3 Transcription Kit (AM1348; Invitrogen), poly(A) tailed with the Poly(A) Tailing Kit (AM1350; Invitrogen). To assess the efficiency of Cas9 mRNA and sgRNA, genomic DNA was amplified by PCR and analyzed with T7 endonuclease I (M0302L; NEB). The sgRNAs were coinjected with Cas9 mRNA into one-cell-stage zebrafish embryos. Identified founder F0 zebrafish were crossed with wild-type zebrafish, and germline transmission resulted in the propagation of a stable KO line. To obtain *slc45a2* heterozygous KO zebrafish for the study, we crossed the albino KO fish with wild-type zebrafish. Detailed sgRNA sequences used for generating the *slc45a2* KO mutants are provided in Supplementary Table S3.

Microinjection of mRNA and Plasmid DNAs in Zebrafish

The rescue experiments were performed using synthesized mRNA or plasmid DNA microinjection. *SLC45A2* or *SLC45A2*(W74R) mRNA was transcribed using the mMESSAGE mMACHINE SP6 Transcription Kit (AM1340; Thermo Fisher, Waltham, MA) and purified by lithium chloride precipitation following the manufacturer's protocol. For mRNA overexpression, we microinjected *SLC45A2* or *SLC45A2*(W74R) mRNA at a concentration of 500 pg into one-cell-stage embryos obtained from an in-cross of *slc45a2* KO mutant zebrafish. For quality control for microinjection, we coinjected mRNA with phenol red to see that embryos had been successfully injected. We selected out uninjected, unfertilized, and dead embryos before evaluation. The pigmentation phenotype was evaluated at 52 hpf in injected embryos. Although melanophores first appear at 24 hpf, we selected 52 hpf because it corresponds to the developmental stage at which most of the melanophores have completed their migration, specification, and differentiation in zebrafish embryos, allowing more reliable assessment of pigmentation phenotypes.[20] To achieve transient

somatic expression of *SLC45A2* in zebrafish, 50 ng/µL of plasmid DNAs (*cmv:SLC45A2*, *ftyrp1:SLC45A2*, *ftyrp1:ZsGreen1-P2A-SLC45A2*, or *ftyrp1:ZsGreen1-P2A-SLC45A2*(W74R)) was microinjected into one-cell-stage zebrafish embryos. After injection, embryos were maintained in egg water at 28.5°C until further analysis.

Results

Clinical Description

A 3-year-old male child visited the clinic with infantile nystagmus, esotropia, skin hypopigmentation, and brown hair, initially seeking evaluation for nystagmus. He was born via normal spontaneous vaginal delivery with no perinatal complications. Notably, his mother had nystagmus, photophobia, and reduced visual acuity, while his brother also had brown hair but no visual symptoms or nystagmus (Fig. 1a). There was no known consanguinity in the family. The proband had no history of bleeding tendencies or frequent infections. Dilated fundus examination showed hypopigmented fundi with no foveal reflex, and nystagmus was noted (Fig. 1b). At age 12, his best-corrected visual acuity was 20/40 in both eyes. Cycloplegic refraction showed severe with-the-rule astigmatism: -sph4.25 -cyl4.50 Axis180 in the right eye and -sph3.50 -cyl5.00 Axis180 in the left eye. Slit-lamp examination revealed iris hypopigmentation (Fig. 1c). Wide-field fundus photography showed a concentric macular ring sign in both eyes, and fundus photographs showed grade 1 macular transparency with visible choroidal vessels. OCT exhibited bilateral grade 2 foveal hypoplasia with intrusion of plexiform layers and an absence of foveal pit, with a minor degree of outer segment lengthening.[19] Multichannel VEP confirmed chiasmal misrouting of the optic nerve (Fig. 2). Both spontaneous and gaze-evoked nystagmus were noted, showing a symmetric 3-Hz bidirectional jerk-type nystagmus.

The mother also had light brown hair and iris hypopigmentation (Fig. 1a). Her best-corrected visual acuity was 20/32 in the right eye and 20/25 in the left eye. Fundus examination revealed a weak foveal reflex, and OCT showed grade 1b foveal hypoplasia (Figs. 2e, 2f). She had undergone four large recti recession surgeries in her early teens to reduce nystagmus. Video nystagmography showed that her nystagmus was minimal in the primary position, but gaze-evoked nystagmus was noted. The brother of the proband also had light brown hair, with a best-corrected visual acuity of 20/20 in both eyes. He did not have nystagmus. OCT revealed grade 1a foveal hypoplasia in both eyes (Figs. 2g, 2h).

Sequencing Analysis and Pathogenicity Prediction

Targeted panel sequencing identified a novel heterozygous c.220T>C:p.(Trp74Arg) variant in the *SLC45A2* gene (NM_016180.5). The c.220T>C:

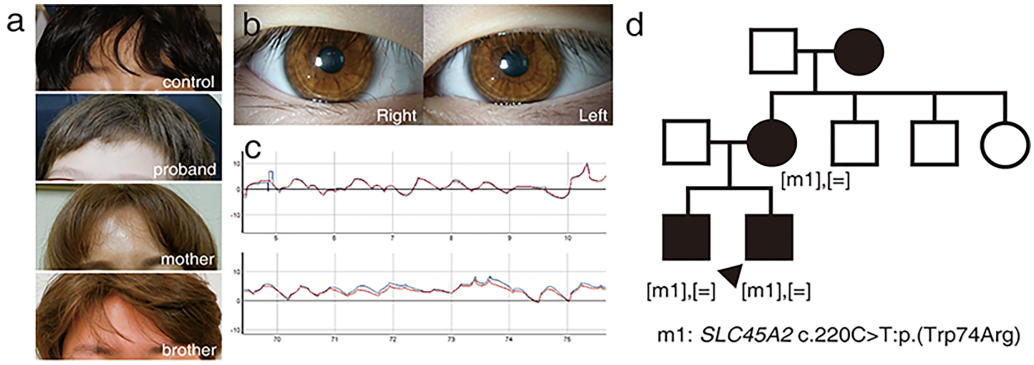

Figure 1. Identification of a novel *SLC45A2*(W74R) variant in a family with autosomal dominant inherited OCA. (**a**) Hair of an age- and sex-matched control of the proband and affected members of the OCA family. Brownish hair was observed in all affected family members, with the proband being the most severely affected. (**b**) Anterior segment photographs of the proband. Iris hypopigmentation was noted in both eyes. (**c**) Video-nystagmography (VNG) result of the proband. The horizontal axis represents time in seconds, and the vertical axis represents eye position in degrees (*upward* indicates rightward movement, and *downward* indicates leftward movement). The VNG recording represents horizontal position changes during spontaneous fixation. A 2- to 3-Hz bilateral symmetric pendular nystagmus was observed (*red line*: right eye; *blue line*: left eye). (**d**) The pedigree revealed a dominant inheritance pattern. Targeted panel sequencing identified a novel heterozygous c.220C>T:p.(Trp74Arg) variant in *SLC45A2*. Sanger sequencing confirmed the variant was segregated in the affected family members. Although we could not examine the affected grandmother, the proband's mother indicated that the grandmother had nystagmus and reduced visual acuity since childhood.

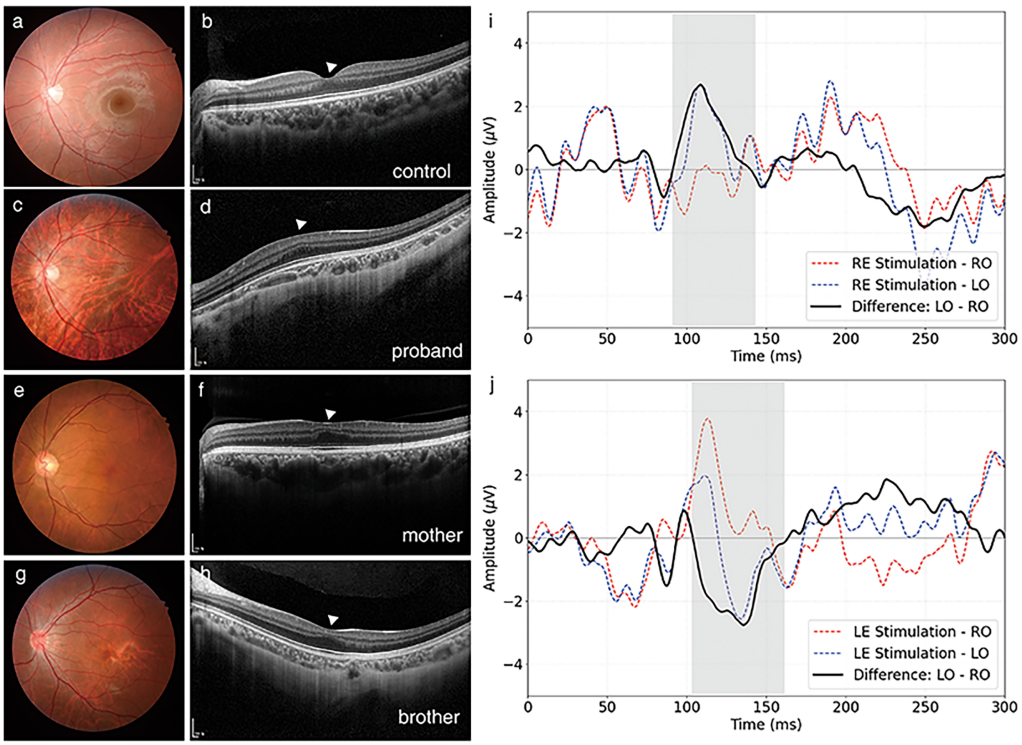

Figure 2. Fundus photographs and OCT images of an age- and sex-matched control of the proband and affected members of the OCA family. (**a, b**) Foveal pigmentation and foveal reflex were observed, and OCT showed a normal foveal pit (*arrowhead*) in an unrelated healthy control subject. These images serve as a reference for comparison with affected family members. (**c, d**) Fundus photography of the proband revealed no foveal reflex, but OCT showed grade 2 foveal hypoplasia. No foveal pit was observed. (**e, f**) Fundus photography of the affected mother showed a weak foveal reflex, and OCT revealed grade 1b fovea hypoplasia. A shallow foveal pit was noted. (**g, h**) Fundus photography of the affected brother showed a weak foveal reflex, and OCT revealed grade 1a foveal hypoplasia. A shallow foveal pit and retention of the inner retinal layer at the fovea center were observed. (**i, j**) Multichannel pattern visual evoked potential (VEP) analysis of the proband. The graphs show waveforms recorded from the right occipital (RO, *red dashed lines*) and left occipital (LO, *blue dashed lines*) electrodes, together with their difference wave (*solid black line*), following pattern stimulation of the right eye (RE) and left eye (LE). The LO–RO difference wave shows a prominent positive peak in the P100 latency region during RE stimulation and a negative peak during LE stimulation, indicating chiasmal misrouting with crossed asymmetry (highlighted in *gray*).

p.(Trp74Arg) variant is absent in gnomAD v4.1, TOGOVAR, and KRGDB and is predicted to be deleterious by multiple in silico tools (Supplementary Table S4; AlphaMissense: 0.993, CADD: 29.6, REVEL: 0.951, and VEST4: 0.965). The REVEL and VEST4 scores are considered PP3 strong.[21] It was also identified in the affected mother and brother (Fig. 1d, Supplementary Fig. S1). The c.220 nucleotide position is highly conserved (PhastCons 1.00 and PhyloP 5.05), and the tryptophan at residue 74 is highly conserved across species from fruit fly to human (Fig. 3a). Structural analysis using AlphaFold3 Server and UCSF ChimeraX v1.8 revealed that the wild-type structure containing Trp74 exhibits a relatively stable local conformation with minimal steric conflicts. In contrast, the W74R substitution compromises local structural integrity due to a significant steric overlap between Arg74 and Tyr70, resulting in a threefold increase in steric clashes (Fig. 3b, Supplementary Table S5). Although the pedigree suggested autosomal dominant inheritance, we searched for all other possible regulatory, deep intronic, or structural variants in all OCA, OA, syndromic OCA genes. However, genome sequencing did not reveal such variants in other OCA-related genes (Supplementary Table S6). Based on imputed haplotype analysis, the c.1122G>C:p.(Leu374Phe) (rs16891982) variant in *SLC45A2*, which is associated with lighter skin, hair, and eye pigmentation, was not detected.[22] All other variants were common polymorphisms or had low CADD scores (all Phred scales <12). Only one deep intronic variant, c.563-5580G>C, had a spliceAI score of 0.12, and the proband was homozygous for this variant. However, this variant has a minor allele frequency of 0.1093 in the gnomAD East Asian population, with a total of 238 homozygous allele counts, making it unlikely to be causative. Other reported polymorphisms in *SLC45A2* (rs181832,

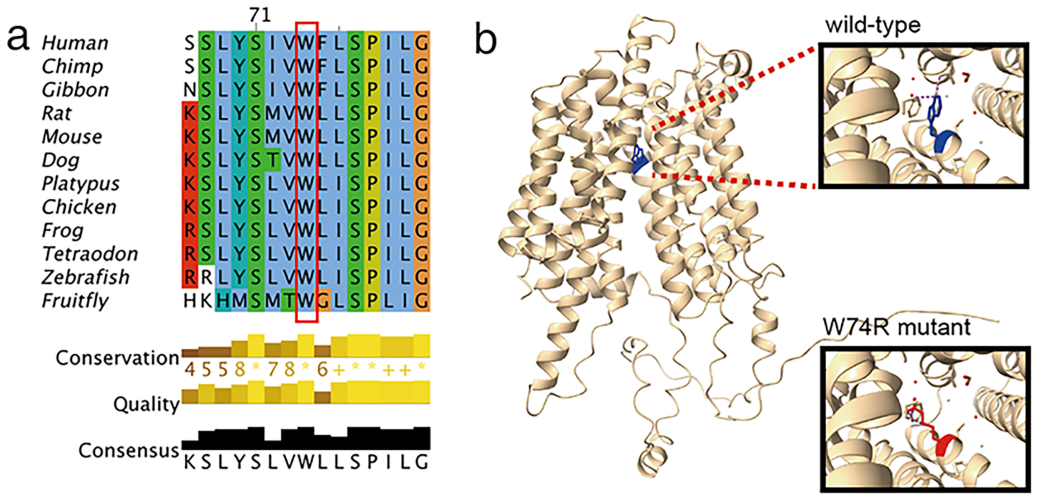

Figure 3. Comparison of SLC45A2 proteins from different species and molecular modeling of the *SLC45A2*(W74R) variant. (**a**) Evolutionary conservation of tryptophan (W) at position 74, from fruit fly to human. The W74R mutation changes hydrophobic tryptophan to positively charged, hydrophilic arginine. (**b**) Molecular modeling using the AlphaFold 3 Server and the protein structure visualization tool UCSF ChimeraX. The W74R mutation introduces a physically impossible overlap with Tyr70, indicating severe structural destabilization.

rs26722, rs2287949, rs35394, rs40132, and rs250417) were also investigated.[23] Notably, alleles associated with blond hair and blue eyes, including rs181832 (T allele), rs2287949 (G allele), and rs250417 (G allele), were not observed (Supplementary Table S7). The common hypomorphic c.575C>A:p.(Ser192Tyr) and c.1205G>A:p.(Arg402Gln) variants in *TYR*, which are associated with fair skin color, were not detected in the proband.[14] The regulatory c.-301C>T variant was also not observed.[24] Additionally, the known pathogenic regulatory c.-492_-489del or c.-1078_-1077del variants in *SLC45A*2 were not detected.[25,26] Although this variant has been submitted to LOVD (#0000794070) and previously reported by our group,[27] a detailed description of the phenotypes and functional validation has not yet been conducted.

Generation of *slc45a2* KO Zebrafish and Rescue Experiments

To assess the pathogenicity of the human *SLC45A2*(W74R) variant, we generated *slc45a2* KO zebrafish. Genomic DNA sequencing identified a 14-bp deletion and an 18-bp deletion in exon 1 of the *slc45a2* gene in KO zebrafish, resulting in a frameshift mutation (Supplementary Table S8). The frameshift mutation is predicted to cause the loss of transmembrane domains of the Slc45a2 protein (Fig. 4a). *slc45a2* KO zebrafish showed a typical albino phenotype without any other global developmental defects (Figs. 4b, 4c), consistent with previous reports.[28,29] We initially performed a rescue experiment using mRNA overexpression. This approach is widely used for the functional validation of human variants in zebrafish and useful for studying the effects of dominant variants by potentially allowing the assessment of the mutant protein's function in the presence of the endogenous wild-type protein.[30–32] We performed microinjection of *SLC45A2* or *SLC45A2*(W74R) mRNA at a concentration of 500 pg per embryo at the one-cell stage and evaluated the pigmentation phenotype at 52 hpf (Supplementary Table S2). However, no significant change was observed in *SLC45A2* mRNA-injected KO zebrafish compared to uninjected KO zebrafish (Fig. 4d). Phenotypic change was not observed in *SLC45A2*(W74R) mRNA-injected KO zebrafish (data not shown). Similar results were obtained in wild-type zebrafish injected with *SLC45A2* or *SLC45A2*(W74R) mRNA (Figs. 4e–g). There was no significant difference in normal development and pigmentation between uninjected and injected wild-type or KO zebrafish, consistent with previous reports.[28,29] These results suggest that mRNA overexpression is not a reliable method for functional validation of *SLC45A2* variants in zebrafish, possibly due to mRNA or protein instability. In the previous study, however, the rescue experiment, which involved the injection of a Bacterial Artificial Chromosome (BAC) clone, showed an obvious pigmentation phenotype in *slc45a2* KO zebrafish. The BAC clone (CR749169, ~169 kb) contains the complete coding sequence of the zebrafish *slc45a2* gene along with the necessary regulatory elements

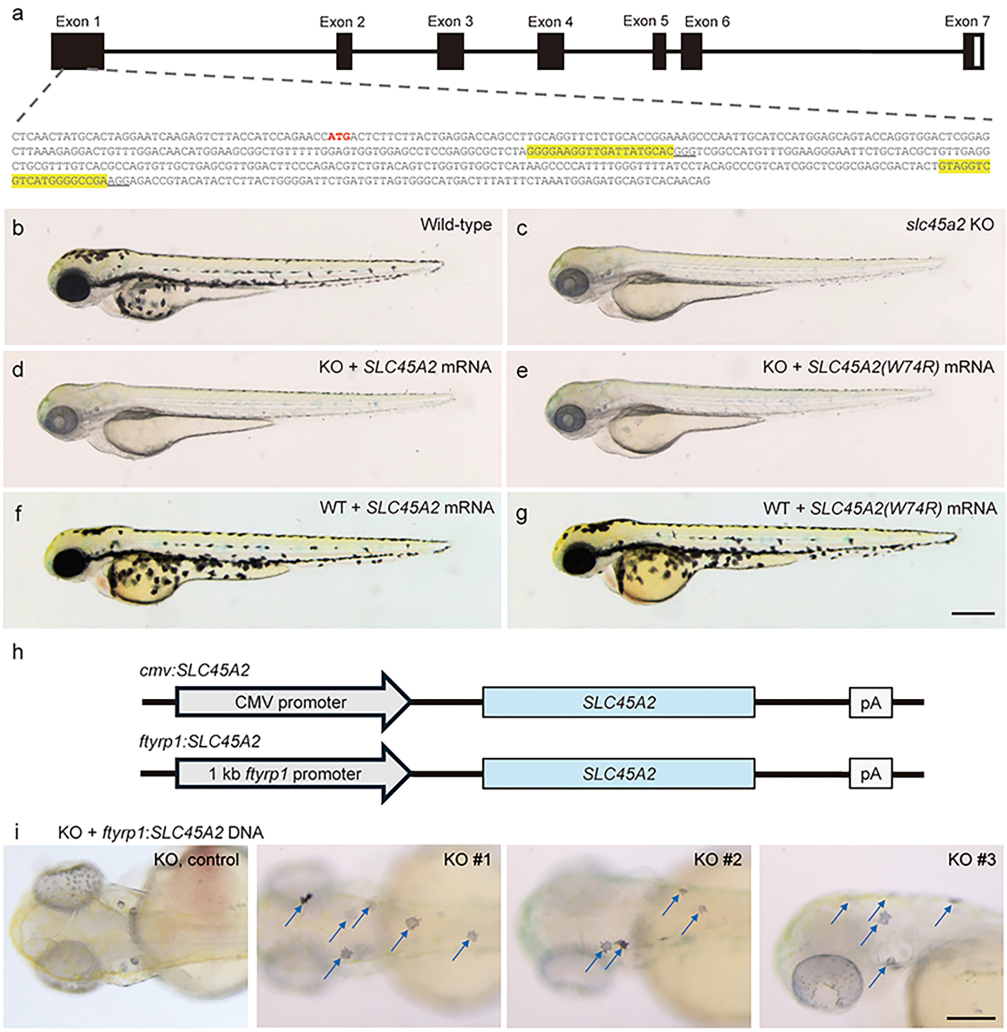

Figure 4. Establishment of *slc45a2* KO zebrafish and effects of overexpression of *SLC45A2* or *SLC45A2*(W74R) mRNA in KO zebrafish. (**a**) Schematic view of the zebrafish *slc45a2* gene structure and CRISPR target site in exon 1 (*arrow*). Predicted protein structure resulted from the frameshift mutation in *slc45a2* KO zebrafish. Multiple transmembrane domains in the wild-type (WT) Slc45a2 protein are marked in *gray*. (**b, e**) Wild-type zebrafish at 52 hpf ($n = 20$). (**c**) Uninjected control KO zebrafish ($n = 20$). (**d**) *SLC45A2* mRNA-injected KO zebrafish ($n = 20$). (**f**) *SLC45A2* mRNA-injected WT zebrafish ($n = 20$). (g) *SLC45A2*(W74R) mRNA-injected WT zebrafish ($n = 20$). (**h**) Schematic view of *SLC45A2* expression vectors under control of the *cmv* promoter or melanocyte-specific *ftyrp1* promoter. (**i**) Detection of rescued melanocytes (*arrows*) in representative individual KO zebrafish (KO 1–3, $n = 15$; KO control, $n = 4$) at 72 hpf after injection with *ftyrp1:SLC45A2* plasmid DNA. Five to seven positive melanocytes were detected in an individual KO zebrafish. *Scale bar*: 400 µm.

required to drive its tissue-specific expression in the melanocytes.[26]

Melanocyte-Specific Expression of Transgene Using the *ftyrp1* Promoter

To achieve a more stable and consistent expression of *SLC45A2*, we injected plasmid DNA of the expression vector. We used the CS2$^+$ vector, a general multipurpose expression vector in which transgene expression is regulated by the cytomegalovirus (*cmv*) promoter (Fig. 4h). However, no rescued melanocytes were observed in KO zebrafish injected with this vector (data not shown, $n = 15$). We hypothesized that the *cmv* promoter, although widely considered constitutive, might not be effectively expressed in differentiated melanocytes. Notably, *slc45a2* transcription is specifically expressed in migrating neural crest cells and differentiating melanocytes (Supplementary Fig. S2). To overcome this limitation, we used a tissue-specific promoter, tyrosinase-related protein 1 (*ftyrp1*) gene promoter, which is known to have melanocyte-specific expression in fish.[33] This approach led to the success-

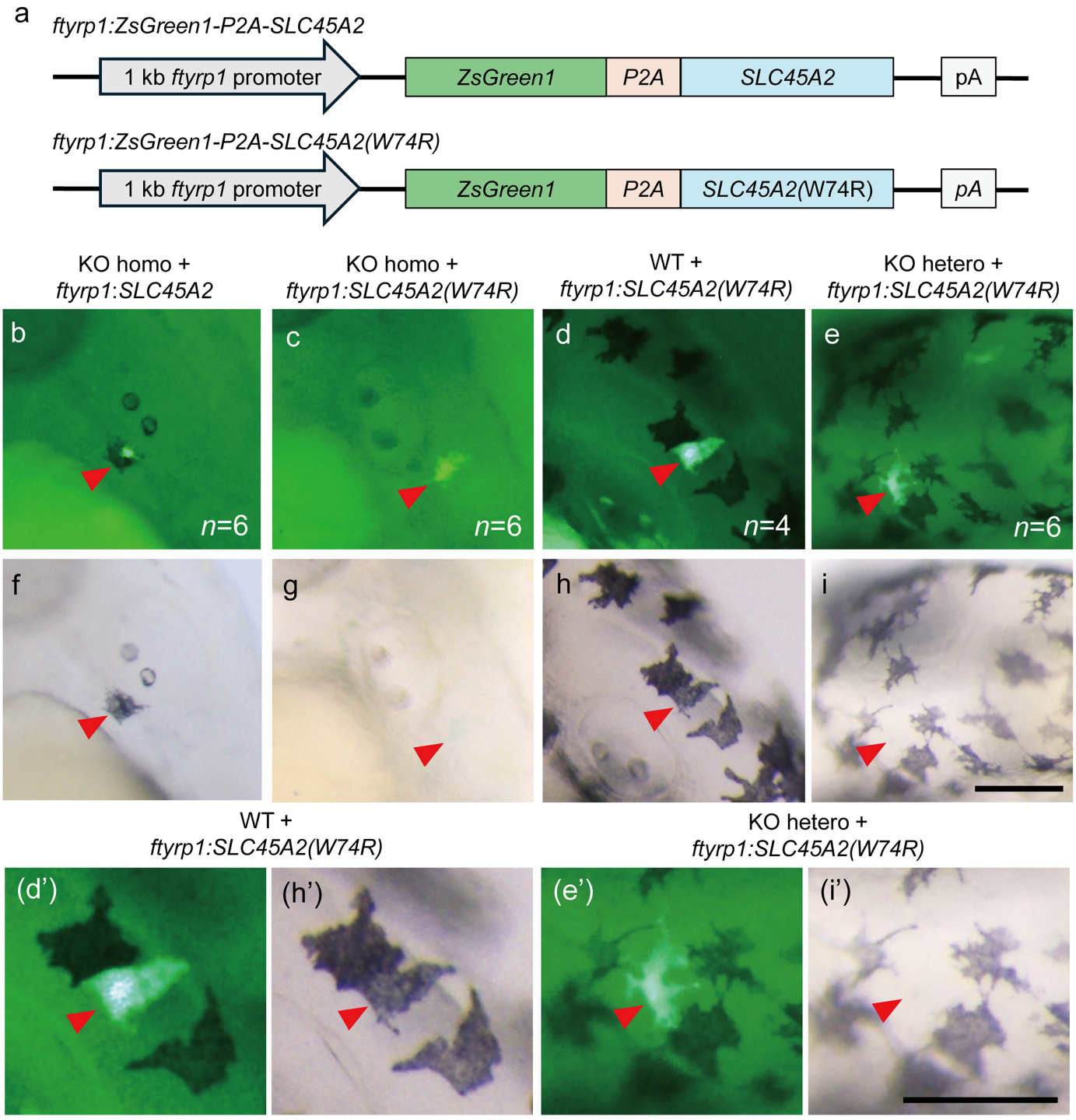

Figure 5. Dominant-negative and dosage effects of *SLC45A2*(W74R) expression in melanocyte-specific transgenic zebrafish. (**a**) Schematic view of *SLC45A2* or *SLC45A2*(W74R) expression vector under control of the melanocyte-specific *ftyrp1* gene promoter. ZsGreen1 is used as a fluorescent reporter for the transgene-positive cells (*arrowheads*). (**b, f**) Rescue effects of human *SLC45A2* in *slc45a2* KO zebrafish at 48 hpf. ZsGreen1-positive melanocytes are detected in homozygous *slc45a2* KO (KO homo, −/−, $n = 6$). (**c, g**) No rescue effect of *SLC45A2*(W74R) in ZsGreen1-positive cells in KO homo ($n = 6$). (**d, h, d', h'**) No effect of *SLC45A2*(W74R) in wild-type zebrafish (WT, +/+). ZsGreen1 is expressed in normal melanocytes in WT ($n = 4$). (**e, i, e', i'**) Dominant-negative effects of *SLC45A2*(W74R) in heterozygous *slc45a2* KO (KO hetero, +/−). ZsGreen1-positive melanocytes are not detected in KO hetero ($n = 6$). (**b–e, d', e'**) Fluorescent images. (**f–i, h', i'**) Bright-field images. (**d', e', h', i'**) Magnifications of arrow-marked cells in d, e, h, and i, respectively. *Scale bar*: 100 µm.

ful rescue of melanocytes in *slc45a2* KO zebrafish injected with the *ftyrp1:SLC45A2* expression vector (Fig. 4i). These results highlight that tight control of gene expression in proper time and space in a specific tissue is necessary for the functional validation of human *SLC45A2* variants in *slc45a2* KO zebrafish.

Dominant-Negative Activity of *SLC45A2*(W74R) in Heterozygous KO Zebrafish

After the successful rescue experiment using melanocyte-specific promoter-driven *SLC45A2* expression in KO zebrafish, we next sought to validate the functional impact of the *SLC45A2*(W74R) variant using the same approach. To monitor gene expression and rescue activity at the single-cell level in a mosaic pattern in transiently transgenic zebrafish, we introduced a fluorescent reporter system using ZsGreen1. We constructed a *ZsGreen1-P2A-SLC45A2* double expression vector under the control of the *ftyrp1* promoter (Fig. 5a). To refine expression control, we introduced the 2A peptide system, which can induce ribosomal skipping during translation and produce two independent proteins, rather than a fusion protein. This vector construct enabled the simultaneous expression of the *ZsGreen1* reporter and target gene specifically in melanocytes, allowing us to evaluate the effects of *SLC45A2* or *SLC45A2* variants at the cellular level.

To examine the rescue ability of *SLC45A2*, we microinjected *ftyrp1:ZsGreen1-P2A-SLC45A2* plasmid into *slc45a2* KO zebrafish and observed the pigmentation phenotype at 48 hpf. ZsGreen1-positive melanocyte expressing *SLC45A2* rescued the albino phenotype (Figs. 5b, 5f), indicating the effectiveness of the mosaic expression method using the *ftyrp1* promoter for the functional validation of the *SLC45A2* variant. Next, we injected the *ftyrp1:ZsGreen1-P2A-SLC45A2*(W74R) plasmid into *slc45a2* KO zebrafish but observed no pigmentation phenotype, suggesting that the *SLC45A2*(W74R) variant disrupts normal *SLC45A2* function (Figs. 5c, 5g).

To further investigate the effect of the *SLC45A2*(W74R) variant, we introduced the *ftyrp1:ZsGreen1-P2A-SLC45A2*(W74R) plasmid into *slc45a2* heterozygous KO zebrafish. Interestingly, melanin synthesis was completely inhibited in ZsGreen1-positive melanocytes expressing *SLC45A2*(W74R), while ZsGreen1-negative melanocytes exhibited normal melanin synthesis (Figs. 5d, 5e, 5h, 5i). We also tested the known *SLC45A2*(Y70H) variant using the same assay system and observed similar results (Supplementary Fig. S3), indicating that both Y70H and W74R variants can act in an autosomal dominant manner. Taken together, our results suggest that melanocyte-specific expression of the *SLC45A2*(Y70H) or *SLC45A2*(W74R) variant recapitulates the patient's phenotype in zebrafish, supporting the pathogenicity of these autosomal dominant variants in *SLC45A2*.

Discussion

In this study, we report a novel dominant variant in *SLC45A2*, causing autosomal dominant OCA4 in three patients from a single family. The *SLC45A2*(W74R) variant was absent in gnomAD v4.1, and no other candidate genetic causes were identified. Genome sequencing revealed no rare single-nucleotide variants, indels, structural variants, or mobile element insertions in known OCA genes. Melanocyte-specific expression of the *SLC45A2*(W74R) variant in heterozygous KO zebrafish recapitulated the patient's phenotype, showing impaired melanogenesis. Therefore, *SLC45A2* can be inherited in either an autosomal dominant or recessive manner, depending on the mutation.[8,9]

A recent study identified a de novo c.628C>T:p.(Arg210Cys) variant in *TPCN2* as a cause of skin hypopigmentation without eye abnormalities.[34] The affected proband had normal visual acuity, foveal structure, and retinal pigmentation with no signs of nystagmus. Therefore, this individual does not meet the diagnostic criteria for OCA. Similarly, a gain-of-function of chloride channel 7 (*CLCN7*) Tyr715Cys variant has been reported to induce cutaneous hypopigmentation, developmental delay, organomegaly, and lysosomal storage.[35] However, in patients with dominant *CLCN7* variants, no hypopigmentation was observed in either the iris or retina, which is inconsistent with typical OCA. Since melanosomal pH is a key regulator in melanin synthesis, a dominant variant in *TPCN2* or *CLCN7* may disrupt the ability to neutralize pH in melanosome in patient melanocytes.

Another autosomal dominant form of OCA4, the c.208T>C:p.(Tyr70His) *SLC45A2* variant, *SLC45A2*(Y70H), was suggested in a family without genome sequencing and functional study.[4] Both *SLC45A2*(Y70H) and *SLC45A2*(W74R) mutations are located in the second transmembrane domain, which is highly conserved and positioned near a crucial motif found in major facilitator superfamily (MFS) transporters.[36] This motif, termed motif-A, is located between the second and third transmembrane

helices on the cytoplasmic side and plays a crucial role in cytoplasmic gating. Several studies on motif-A in different MFS transporters have shown that changes in this region often hinder the transporter's function.[37–39] Since the transmembrane domains are embedded in the lipid bilayer, the amino acid residues in this domain are typically hydrophobic. These two dominant variants replace hydrophobic residues with hydrophilic amino acids, which is thought to disrupt SLC45A2 function. In contrast, c.217G>T:p.(Val73Leu) and c.217G>A:p.(Val73Met) variants have been reported to follow an autosomal recessive pattern.[40,41] These mutations likely have a less pathogenic effect, as both valine and leucine are hydrophobic, and methionine is amphipathic. Further studies are needed to explore the detailed molecular mechanism of *SLC45A2*(Y70H) and *SLC45A2*(W74R) variants.

In the *slc45a2* KO zebrafish model, melanocyte-specific expression of *SLC45A2*(W74R) failed to rescue pigmentation phenotype in a homozygous (–/–) KO zebrafish model, whereas wild-type *SLC45A2* successfully rescued the phenotype. Conversely, *SLC45A2*(W74R) showed an inhibitory effect on pigmentation in heterozygous (+/−) KO zebrafish, suggesting a dominant-negative mode of action. Furthermore, *SLC45A2*(W74R) did not significantly affect pigmentation in wild-type (+/+) zebrafish, suggesting a dosage effect due to competition with the theoretically double amount of endogenous Slc45a2 proteins in the wild-type zebrafish.

We speculate that this finding can be explained by a dosage-sensitive, dominant-negative mechanism with a buffering effect exerted by the excess wild-type SLC45A2 protein. In wild-type zebrafish, the high concentration of endogenous SLC45A2 may outcompete or sequester the mutant protein, thereby preventing its inhibitory influence. However, when the relative dosage of the mutant allele surpasses this buffering threshold, dominant-negative interference emerges, resulting in pigment loss. This threshold-dependent behavior is consistent with the gene dosage balance model described by Veitia and Birchler,[42] in which nonlinear genotype–phenotype relationships allow partial functional compensation above a critical protein concentration.

However, the degree of a dominant-negative effect in the KO zebrafish model differs slightly from that observed in human *SLC45A2*(W74R) patients. In patients, the pigmentation phenotype is milder and more variable than in the KO zebrafish model. We hypothesize that the melanocyte-specific promoter, *ftyrp1*, used in this study may be stronger than the *SLC45A2* gene promoter in humans. This hypothesis also supports the idea that variable expressivity in human patients could be due to different genomic backgrounds and a complex interplay of multiple genetic factors.

It is interesting to note the variable clinical features within this family with OCA4. Both the proband and the mother exhibited light brown hair, iris hypopigmentation, and infantile nystagmus, but the mother exhibited a milder phenotype as she did not have fair skin and had better visual acuity, less photophobia, and a lower grade of foveal hypoplasia. The affected brother had brown hair but nearly normal skin pigmentation. He had minimal foveal hypoplasia (grade 1a), demonstrated 20/20 vision in both eyes, and showed no signs of nystagmus.

Variable expression is typically more common in dominant conditions than in recessive ones, with the degree of hypopigmentation varying from mild to severe. Hair color can range from white to yellow, blond, and brown, while iris pigmentation may range from gray to blue-gray to brown. The variable expressivity of the autosomal dominant *SLC45A2* was also described in the case of *SLC45A2*(Y70H).[4] Although it depends on genomic background, the precise mechanism underlying this variability remains unclear. However, recent systematic genetic interaction mapping of the solute carrier (SLC) superfamily has demonstrated that *SLC* genes can interact with other *SLC*s and non-*SLC* genes, resulting in altered cellular phenotypes, including metabolic reprogramming and signaling changes.[43] This suggests that unidentified modifier genes may further influence the phenotypic outcome associated with SLC45A2 variants. Additionally, transcriptional and posttranscriptional regulation, such as microRNA binding site polymorphisms, can also modulate SLC gene expression and contribute to phenotypic variability.[44] It has been reported that variations in *TYR* can influence the expressivity in patients with OCA by serving as a modifier gene.[14] However, the identified polymorphisms c.575C>A:p.(Ser192Tyr) and c.1205G>A:p.(Arg402Gln) in *TYR* were not detected in this family. Nonetheless, this case underscores the diverse phenotypes of OCA, highlighting the importance of genetic testing, a vital diagnostic tool for OCA classification.[45]

This study has several limitations. First, the functional assays were performed using zebrafish as a heterologous model, which, despite its conserved melanogenesis pathway, may not fully recapitulate the complexity of human melanocyte biology. Second, the quantitative evaluation of melanin rescue and dominant-negative effects relied primarily on visual and semiquantitative analyses. Therefore, more comprehensive single-cell–level quantification or

biochemical measurement of melanin content could strengthen these findings. Third, although mosaic expression of *SLC45A2*(W74R) in heterozygous KO zebrafish effectively models the coexistence of mutant and wild-type alleles at the cellular level, we could not establish an exactly similar *SLC45A2*(W74R) mutant zebrafish line. Generating such a line and evaluating its pigmentation phenotype could further strengthen the translational relevance of our findings by providing a more direct comparison with the clinical phenotypes observed in human carriers of the *SLC45A2*(W74R) variant. Further studies integrating functional genomics and cell-based assays in human melanocytes are warranted.

In summary, we first functionally validated that both the *SLC45A2*(Y70H) and *SLC45A2*(W74R) mutations can cause OCA in an autosomal dominant manner. As genetic counseling regarding family planning and prenatal testing becomes more prevalent, it is important to understand the inheritance pattern of genetic disorders. Heterozygosity for a dominant-negative variant in *SLC45A2* is not asymptomatic and carries a risk of developing the disorder. Clinicians should be aware that OCA can be inherited in an autosomal dominant manner, particularly in OCA4. Thus, our *ftyrp1* promoter-based rescue experiment will be a valuable tool for the functional validation of new variants in OCA-related genes. Further experimental studies are needed to confirm the pathogenetic mechanism of the dominant-negative effect on these variants.

Acknowledgments

The authors thank the *SLC45A2*-dominant oculocutaneous albinism family for cooperation.

Supported by the National Research Foundation of Korea grant funded by the Korean government (MIST) (grant 2020R1C1C1007965, JH; RS-2024-00349650, C-HK).

Author Contributions: **D.S.**, Formal analysis, Investigation, Writing - Original draft, Writing - Review & Editing; **T.-I.C.**, Formal analysis, Investigation, Writing - Original draft; **J.-W.P.**, Writing - Review & Editing; **D.W.D.**, Writing - Review & Editing; **T.Y.K.**, Data curation, Methodology; **M.G.T.**, Formal analysis (OCT), Writing - Review & Editing; **J.-S.P.**, Writing - Review & Editing; **X.W.**, Resources, Writing - Review & Editing. **Y.-K. B.**, Formal analysis, Writing - Review & Editing; **C.-H.K.**, Conceptualization, Supervision, Writing - Review & Editing, Funding acquisition; **J.H.**, Conceptualization, Supervision, Writing - Review & Editing, Funding acquisition.

Data Availability: All data are available from the corresponding authors upon reasonable request.

Disclosure: **D. Surl**, None; **T.-I. Choi**, None; **J.-W. Park**, None; **D.W. Don**, None; **T.Y. Kim**, None; **M.G. Thomas**, None; **J.-S. Park**, None; **X. Wei**, None; **Y.-K. Bae**, None; **J. Han**, None; **C.-H. Kim**, None

* DS and TIC contributed equally to this article.

References

1. Pavan WJ, Sturm RA. The genetics of human skin and hair pigmentation. *Annu Rev Genomics Hum Genet*. 2019;20:41–72.
2. Thomas MG, Zippin J, Brooks BP. Oculocutaneous albinism and ocular albinism overview. In: Adam MP, Feldman J, Mirzaa GM, Pagon RA, Wallace SE, Amemiya A, eds. *GeneReviews*. Seattle, WA: University of Washington, Seattle, 2023;1993–2026.
3. Kausar T, Bhatti MA, Ali M, Shaikh RS, Ahmed ZM. OCA5, a novel locus for non-syndromic oculocutaneous albinism, maps to chromosome 4q24. *Clin Genet*. 2013;84(1):91–93.
4. Oki R, Yamada K, Nakano S, et al. A Japanese family with autosomal dominant oculocutaneous albinism type 4. *Invest Ophthalmol Vis Sci*. 2017;58(2):1008–1016.
5. Gronskov K, Ek J, Brondum-Nielsen K. Oculocutaneous albinism. *Orphanet J Rare Dis*. 2007;2:43.
6. Kuht HJ, Maconachie GDE, Han J, et al. Genotypic and phenotypic spectrum of foveal hypoplasia: a multicenter study. *Ophthalmology*. 2022;129(6):708–718.
7. Hong ES, Zeeb H, Repacholi MH. Albinism in Africa as a public health issue. *BMC Public Health*. 2006;6:212.
8. Inagaki K, Suzuki T, Shimizu H, et al. Oculocutaneous albinism type 4 is one of the most common types of albinism in Japan. *Am J Hum Genet*. 2004;74(3):466–471.
9. Inagaki K, Suzuki T, Ito S, et al. OCA4: evidence for a founder effect for the p.D157N mutation of the MATP gene in Japanese and Korean. *Pigment Cell Res*. 2005;18(5):385–388.
10. Newton JM, Cohen-Barak O, Hagiwara N, et al. Mutations in the human orthologue of the mouse underwhite gene (uw) underlie a new form of ocu-

locutaneous albinism, OCA4. *Am J Hum Genet*. 2001;69(5):981–988.
11. Bin BH, Bhin J, Yang SH, et al. Membrane-associated transporter protein (MATP) regulates melanosomal pH and influences tyrosinase activity. *PLoS One*. 2015;10(6):e0129273.
12. Lowther C, Valkanas E, Giordano JL, et al. Systematic evaluation of genome sequencing for the diagnostic assessment of autism spectrum disorder and fetal structural anomalies. *Am J Hum Genet*. 2023;110(9):1454–1469.
13. Gardner EJ, Lam VK, Harris DN, et al. The Mobile Element Locator Tool (MELT): population-scale mobile element discovery and biology. *Genome Res*. 2017;27(11):1916–1929.
14. Jagirdar K, Smit DJ, Ainger SA, et al. Molecular analysis of common polymorphisms within the human Tyrosinase locus and genetic association with pigmentation traits. *Pigment Cell Melanoma Res*. 2014;27(4):552–564.
15. Richards S, Aziz N, Bale S, et al. Standards and guidelines for the interpretation of sequence variants: a joint consensus recommendation of the American College of Medical Genetics and Genomics and the Association for Molecular Pathology. *Genet Med*. 2015;17(5):405–424.
16. Rentzsch P, Witten D, Cooper GM, Shendure J, Kircher M. CADD: predicting the deleteriousness of variants throughout the human genome. *Nucleic Acids Res*. 2019;47(D1):D886–D894.
17. Pettersen EF, Goddard TD, Huang CC, et al. UCSF ChimeraX: Structure visualization for researchers, educators, and developers. *Protein Sci*. 2021;30(1):70–82.
18. Yang MY, Zhong JD, Li X, et al. SEAD reference panel with 22,134 haplotypes boosts rare variant imputation and genome-wide association analysis in Asian populations. *Nat Commun*. 2024;15(1):10839.
19. Thomas MG, Kumar A, Mohammad S, et al. Structural grading of foveal hypoplasia using spectral-domain optical coherence tomography a predictor of visual acuity? *Ophthalmology*. 2011;118(8):1653–1660.
20. Lister JA. Development of pigment cells in the zebrafish embryo. *Microsc Res Tech*. 2002;58(6):435–441.
21. Pejaver V, Byrne AB, Feng BJ, et al. Calibration of computational tools for missense variant pathogenicity classification and ClinGen recommendations for PP3/BP4 criteria. *Am J Hum Genet*. 2022;109(12):2163–2177.
22. Yuasa I, Umetsu K, Harihara S, et al. Distribution of the F374 allele of the SLC45A2 (MATP) gene and founder-haplotype analysis. *Ann Hum Genet*. 2006;70(pt 6):802–811.
23. Cerqueira CC, Hunemeier T, Gomez-Valdes J, et al. Implications of the admixture process in skin color molecular assessment. *PLoS One*. 2014;9(5):e96886.
24. Michaud V, Lasseaux E, Green DJ, et al. The contribution of common regulatory and protein-coding TYR variants to the genetic architecture of albinism. *Nat Commun*. 2022;13(1):3939.
25. Okamura K, Hayashi M, Nakajima O, et al. A 4-bp deletion promoter variant (rs984225803) is associated with mild OCA4 among Japanese patients. *Pigment Cell Melanoma Res*. 2019;32(1):79–84.
26. Rooryck C, Morice-Picard F, Elcioglu NH, Lacombe D, Taieb A, Arveiler B. Molecular diagnosis of oculocutaneous albinism: new mutations in the OCA1-4 genes and practical aspects. *Pigment Cell Melanoma Res*. 2008;21(5):583–587.
27. Moon D, Park HW, Surl D, et al. Precision medicine through next-generation sequencing in inherited eye diseases in a Korean cohort. *Genes (Basel)*. 2021;13(1):27.
28. Tsetskhladze ZR, Canfield VA, Ang KC, et al. Functional assessment of human coding mutations affecting skin pigmentation using zebrafish. *PLoS One*. 2012;7(10):e47398.
29. Dooley CM, Schwarz H, Mueller KP, et al. Slc45a2 and V-ATPase are regulators of melanosomal pH homeostasis in zebrafish, providing a mechanism for human pigment evolution and disease. *Pigment Cell Melanoma Res*. 2013;26(2):205–217.
30. Lee YR, Kim SH, Ben-Mahmoud A, et al. Eif2b3 mutants recapitulate phenotypes of vanishing white matter disease and validate novel disease alleles in zebrafish. *Hum Mol Genet*. 2021;30(5):331–342.
31. Lee YR, Khan K, Armfield-Uhas K, et al. Mutations in FAM50A suggest that Armfield XLID syndrome is a spliceosomopathy. *Nat Commun*. 2020;11(1):3698.
32. Wongkittichote P, Choi TI, Kim OH, et al. Expanding allelic and phenotypic spectrum of ZC4H2-related disorder: a novel hypomorphic variant and high prevalence of tethered cord. *Clin Genet*. 2023;103(2):167–178.
33. Zou J, Beermann F, Wang J, Kawakami K, Wei X. The Fugu tyrp1 promoter directs specific GFP expression in zebrafish: tools to study the RPE and the neural crest-derived melanophores. *Pigment Cell Res*. 2006;19(6):615–627.
34. Wang Q, Wang Z, Wang Y, et al. A gain-of-function TPC2 variant R210C increases affinity

to PI(3,5)P(2) and causes lysosome acidification and hypopigmentation. *Nat Commun*. 2023;14(1):226.
35. Nicoli ER, Weston MR, Hackbarth M, et al. Lysosomal storage and albinism due to effects of a de novo CLCN7 variant on lysosomal acidification. *Am J Hum Genet*. 2019;104(6):1127–1138.
36. Quistgaard EM, Low C, Guettou F, Nordlund P. Understanding transport by the major facilitator superfamily (MFS): structures pave the way. *Nat Rev Mol Cell Biol*. 2016;17(2):123–132.
37. Jiang D, Zhao Y, Wang X, et al. Structure of the YajR transporter suggests a transport mechanism based on the conserved motif A. *Proc Natl Acad Sci USA*. 2013;110(36):14664–14669.
38. Yamaguchi A, Someya Y, Sawai T. Metal-tetracycline/H+ antiporter of Escherichia coli encoded by transposon Tn10. The role of a conserved sequence motif, GXXXXRXGRR, in a putative cytoplasmic loop between helices 2 and 3. *J Biol Chem*. 1992;267(27):19155–19162.
39. Jessen-Marshall AE, Paul NJ, Brooker RJ. The conserved motif, GXXX(D/E)(R/K)XG[X](R/K)(R/K), in hydrophilic loop 2/3 of the lactose permease. *J Biol Chem*. 1995;270(27):16251–16257.
40. Okamura K, Araki Y, Abe Y, et al. Genetic analyses of oculocutaneous albinism types 2 and 4 with eight novel mutations. *J Dermatol Sci*. 2016;81(2):140–142.
41. Kessel L, Kjer B, Lei U, Duno M, Grønskov K. Genotype-phenotype associations in Danish patients with ocular and oculocutaneous albinism. *Ophthalmic Genet*. 2021;42(3):230–238.
42. Veitia RA, Birchler JA. Dominance and gene dosage balance in health and disease: why levels matter! *J Pathol*. 2010;220(2):174–185.
43. Wolf G, Leippe P, Onstein S, et al. The genetic interaction map of the human solute carrier superfamily. *Mol Syst Biol*. 2025;21(6):531–559.
44. Bendova P, Pardini B, Susova S, et al. Genetic variations in microRNA-binding sites of solute carrier transporter genes as predictors of clinical outcome in colorectal cancer. *Carcinogenesis*. 2021;42(3):378–394.
45. Suzuki T, Tomita Y. Recent advances in genetic analyses of oculocutaneous albinism types 2 and 4. *J Dermatol Sci*. 2008;51(1):1–9.